Glia. Author manuscript; available in PMC 2016 May 02.

Published in final edited form as:

Glia. 2013 February ; 61(2): 164–177. doi:10.1002/glia.22424.

Conditional *Sox9* Ablation Reduces Chondroitin Sulfate Proteoglycan Levels and Improves Motor Function Following Spinal Cord Injury

WILLIAM M. MCKILLOP[1,2], **MAGDALENA DRAGAN**[1], **ANDREAS SCHEDL**[3], and **ARTHUR BROWN**[1,2,*]

[1]Robarts Research Institute, University of Western Ontario, London, Ontario, Canada

[2]Department of Anatomy and Cell Biology, University of Western Ontario, London, Ontario, Canada

[3]INSERM U636, Centre de Biochimie, University of Nice/Sophia-Antipolis, Nice, France

Abstract

Chondroitin sulfate proteoglycans (CSPGs) found in perineuronal nets and in the glial scar after spinal cord injury have been shown to inhibit axonal growth and plasticity. Since we have previously identified SOX9 as a transcription factor that upregulates the expression of a battery of genes associated with glial scar formation in primary astrocyte cultures, we predicted that conditional *Sox9* ablation would result in reduced CSPG expression after spinal cord injury and that this would lead to increased neuroplasticity and improved locomotor recovery. Control and *Sox9* conditional knock-out mice were subject to a 70 kdyne contusion spinal cord injury at thoracic level 9. One week after injury, *Sox9* conditional knock-out mice expressed reduced levels of CSPG biosynthetic enzymes (*Xt-1* and *C4st),* CSPG core proteins (brevican, neurocan, and aggrecan), collagens 2a1 and 4a1, and *Gfap,* a marker of astrocyte activation, in the injured spinal cord compared with controls. These changes in gene expression were accompanied by improved hind limb function and locomotor recovery as evaluated by the Basso Mouse Scale (BMS) and rodent activity boxes. Histological assessments confirmed reduced CSPG deposition and collagenous scarring at the lesion of *Sox9* conditional knock-out mice, and demonstrated increased neurofilament-positive fibers in the lesion penumbra and increased serotonin immunoreactivity caudal to the site of injury. These results suggest that SOX9 inhibition is a potential strategy for the treatment of SCI.

Keywords

SOX9; spinal cord injury; neuroplasticity; CSPG; regeneration; perineuronal nets

*Correspondence to: Arthur Brown, Robarts Research Institute, Schulich School of Medicine, University of Western Ontario, 100 Perth Drive, London, Ontario, Canada N6A 5K8. abrown@robarts.ca.

A.B. holds a provisional patent application on SOX9 inhibition as a target for regeneration in the nervous system. No competing financial interests exist for W.M.M., M.D., A.P or A.S.

Additional Supporting Information may be found in the online version of this article.

INTRODUCTION

Damaged axons have a limited capacity for regeneration following adult mammalian spinal cord injury (SCI) (David and Lacroix, 2003). This limited capacity for repair has been attributed, in part, to the nonpermissive environment of the glial scar that forms in the penumbra surrounding the lesion site (Bahr et al., 1995; Davies et al., 1999; Fawcett and Asher, 1999; McKeon et al., 1991; Reier and Houle, 1988). This glial scar is predominantly formed from extracellular matrix (ECM) molecules expressed by reactive astrocytes although macrophages, microglia, oligodendrocytes, invading Schwann cells and meningeal fibroblasts all contribute to production of the scar matrix (Fawcett and Asher, 1999). Chief of the many ECM molecules that serve to inhibit axonal regeneration are the chondroitin sulfate proteoglycans (CSPGs) (Eddleston and Mucke, 1993; Silver and Miller, 2004) that experience a great increase in expression following SCI (Lemons et al., 1999; McKeon et al., 1991). Both *in vitro* and *in vivo* studies have shown that axons do not extend into CSPG-rich ECM (Davies et al., 1997, 1999; McKeon et al., 1991; Meiners et al., 1995; Zuo et al., 1998), and specific CSPGs that inhibit neurite outgrowth have been identified including: aggrecan (Condic et al., 1999), neurocan (Friedlander et al., 1994), phosphocan (Milev et al., 1994), brevican (Yamada et al., 1997), versican (Schmalfeldt et al., 2000), and NG2 (Dou and Levine, 1994).

Strategies designed to target CSPGs at the spinal lesion have resulted in improved axonal regeneration after SCI. Enzymatic digestion of the chondroitin sulfate side chains found on all CSPGs by intrathecal chondroitinase ABC treatment resulted in increased regeneration of ascending and descending tracts after SCI (Bradbury et al., 2002). The combination of chondroitinase ABC with peripheral nerve grafts (Alilain et al., 2011; Houle et al., 2006), rehabilitation (Garcia-Alias et al., 2009; Wang et al., 2011), or neural precursor cell transplantation (Karimi-Abdolrezaee et al., 2010) have all led to improved axonal regeneration and recovery.

We have previously argued that genes with related function are regulated together as classes or batteries after SCI (Gris et al., 2003) and that, in astrocytes, genes that promote axon regeneration and genes that inhibit axon regeneration would be regulated as gene classes. Using bioinformatics we identified putative binding sites for the transcription factor SOX9 (sex-determining region Y-box 9) in the promoter sequences of *Xt-1, Xt-2,* and *C4st-1* in rats, mice and humans. We subsequently used gain of function and loss of function experiments to demonstrate that SOX9 positively regulates the expression of *Xt-1, Xt-2,* and *C4st-1* in primary astrocyte cultures (Gris et al., 2007). Thus we hypothesized that conditional ablation of *Sox9* in mice would result in reduced expression of CSPGs and improved recovery after SCI. We herein report improved hindlimb locomotor recovery after SCI in a line of conditional *Sox9* knock-out mice that correlates with reduced expression of CSPGs and related ECM proteins in the lesion penumbra and at sites more distant to the lesion epicenter.

MATERIALS AND METHODS

Mouse Breeding and *Sox9* Conditional Knock-Out

Conventional *Sox9* knock-out mice have been generated but are unsuitable for studies of SCI as both *Sox9* knock-out ($Sox9^{-/-}$) and heterozygote ($Sox9^{+/-}$) embryos do not survive to birth (Bi et al., 2001). To evaluate SOX9 loss-of-function after SCI, in a nervous system that developed with normal levels of SOX9 activity, a tamoxifen-inducible conditional *Sox9* knock-out strategy was used. We bred a mouse strain that carries floxed *Sox9* (exons 2 and 3 of *Sox9* surrounded by loxP sites) alleles (Akiyama et al., 2002) ($Sox9^{floxlflox}$) with a transgenic mouse line that expresses Cre recombinase fused to the mutated ligand binding domain of the human estrogen receptor (ER) under the control of a chimeric cytomegalovirus immediate-early enhancer/chicken β-actin promoter (*B6.Cg-Tg(CAG-Cre/Esr1)5Amc/J)* (Hayashi and McMahon, 2002) (Jackson Laboratories, Bar Harbor, ME). The resulting $Sox9^{flox/flox}$*; CAGGCreER (*$Sox9^{flox/flox}$*;Cre)* offspring served as tamoxifen inducible *Sox9* knock-out animals and $Sox9^{flox/flox}$ offspring served as control animals expressing normal levels of SOX9. Animals were genotyped by PCR analysis using the following primers:

$Sox9^{flox}$ allele: 5′-ACACAGCATAGGCTACCTG-3′ and 5′-TGGTAATGAGTCATACACAGTAC-3′.

$Sox9^{wildtype}$ allele: 5′-GGGGCTTGTCTCCTTCAGAG-3′ and 5′-TGGTAATGAGTCATACACAGTAC-3′.

$Sox9^{knock\text{-}out}$ allele: 5′-GTCAAGCGACCCATG-3′ and 5′-TGGTAATGAGTCATACACAGTAC-3′

Cre^{+} allele: 5′-CAATTTACTGACCGTACAC-3′ and 5′-AGCTGGCCCAAATGTTGCTG-3′.

Tamoxifen (Sigma Aldrich, St. Louis, MO) was administered at 3 mg/20 g mouse by oral gavage to all $Sox9^{flox/flox}$*;Cre* and $Sox9^{flox/flox}$ littermates once a day for 7 days. Following the final clay of tamoxifen oral gavage the animals were housed for 7 days without treatment to allow time for Cre-mediated recombination and tamoxifen clearance before subsequent SCI.

Primary Astrocyte Cultures

Primary astrocyte cultures were prepared from newborn $Sox9^{flox/flox}$*;Cre* or $Sox9^{flox/flox}$ control mice at postnatal day 1. The upper portion of the skull was removed and the meninges carefully dissected away to avoid contamination of the culture with fibroblasts. The neocortices were removed, individually placed into serum-free Minimum Essential Medium Eagle (EMEM) (Lonza, Walkersville, MD), homogenized by trituration, and gravity-filtered through a 40-μm cell strainer (Becton Dickinson and Company, Toronto, Ontario, Canada). The cells were plated in EMEM + 20% FBS (Invitrogen, Carlsbad, CA), penicillin/streptomycin (Invitrogen, Carlsbad, CA); each animal's cells were divided into two wells each of a six-well dish (Becton Dickinson and Company, Toronto, Ontario, Canada). After 2 weeks in culture 1 μM 4-hydroxytamoxifen (Sigma Aldrich, St. Louis, MO) was administered in three changes of media over 1 week. Following 4-

hydroxytamoxifen administration the cells were cultured in normal media for 1 more week. The percentage of GFAP-expressing cells in these cultures was found to be >95%.

Real-Time PCR

RNA was extracted from *Sox9* conditional knock-out and *Sox9*-positive control primary astrocyte cultures 1 week post-tamoxifen administration, and from the lesion epicenter of *Sox9* conditional knock-out and *Sox9* positive control mice 1 week post-SCI, using the RNA-Easy kit according to the manufacturer's instructions (Qiagen, Valencia, CA). First strand cDNA was synthesized from 1 μg RNA per sample using the High Capacity cDNA Archive Kit according to the manufacturer's instructions (Applied Biosystems, Carlsbad, CA). TaqMan assays were conducted using the Applied Biosystems gene expression assay primer probe sets listed in Table 1.

TaqMan (Applied Biosystems, Carlsbad, CA) gene expression assays were conducted on a 7900HT fast real-time PCR apparatus (Applied Biosystems, Carlsbad, CA) using thermal cycler conditions set as follows; 10 min at 95°C followed by 40 cycles of 30 s at 95°C followed by 30 s at 60°C. Cycle thresholds (Ct) for all target genes are given in Table 1. A standard curve of cycle thresholds using cDNA serial dilutions was established and used to calculate mRNA expression. Target gene mRNA expression was normalized to the amount of 18S mRNA present in each sample. The ratio of knock-out to control sample normalized target gene mRNA was analyzed by Student's *t*-test.

Western Blotting

Protein was isolated from the lesion site (0.45 cm) in tamoxifen-treated *Sox9* conditional knock-out and *Sox9*-positive control mice 2 weeks post-SCI. The western blot membrane was blocked in 10% nonfat powdered milk and then incubated with primary antibodies; anti-SOX9 (AB 5535, Millipore, Billerica, MA used at 1:1,000), anti-GFAP (MAB360, Millipore, Billerica, MA used at 1:1,000), and anti-β-actin (A1978, Sigma, St. Louis, MO, used at 1:10,000) for protein expression assessed by western blot. HRP conjugated anti-mouse IgG (715-035-151, Jackson ImmunoResearch Laboratories, West Grove, PA) and HRP conjugated anti-rabbit IgG (711-035-152, Jackson ImmunoResearch Laboratories, West Grove, PA) secondary antibodies were used at 1:20,000 dilution to detect SOX9, GFAP, and β-actin protein expression. SOX9 and GFAP protein expression was normalized to β-actin protein expression by densitometry using the EpiChemi^3 Darkroom (UVP Bioimaging Systems, Upland, CA) and LabWorks software (Media Cybernetics Inc, Bethesda, MD). Protein samples were also loaded in parallel at 3 μg/well into a Bio-Rad Slot-blot apparatus (BioRad, Mississauga, Ontario) and vacuum transferred onto a nitrocellulose membrane (BioRad, Mississauga, Ontario). The membrane was blocked in 10% nonfat powdered milk and then incubated with primary antibody at 1:200 dilution overnight for anti-CS-56 (C8035, Sigma, St. Louis, MO) or 1:10,000 dilution for anti-β-actin (A1978, Sigma, St. Louis, MO). HRP conjugated anti-mouse IgM (62-6820, Invitrogen, Carlsbad, CA) and anti-mouse IgG (715-035-151, Jackson ImmunoResearch Laboratories, West Grove, PA) secondary antibodies were used at 1:20,000 dilutions to detect CS56 and β-actin protein expression. CS56 protein expression was normalized to β-

actin protein expression by densitometry using the EpiChemi^3 Darkroom (UVP Bioimaging Systems, Upland, CA) and LabWorks software (Media Cybernetics Inc, Bethesda, MD).

Spinal Cord Injury

All protocols for these experiments were approved by the University of Western Ontario Animal Care Committee in accordance with the policies established in the Guide to Care and Use of Experimental Animals prepared by the Canadian Council on Animal Care. One week after the last tamoxifen oral gavage, 13 female *Sox9*$^{flox/flox}$;*Cre* and 16 female *Sox9*$^{flox/flox}$ mice were anesthetized with 100 mg/kg ketamine: 5 mg/kg xylazine. The T9 spinal cord segment was exposed by a dorsal laminectomy. The spinal cord was stabilized at T8 and T10 with forceps. The T9 spinal segment was injured by a 70 kdyne contusion delivered with a 1 s dwell time by a computer-controlled Impactor (displacement range: 500–900 μM) (Infinite Horizons Impactor, Precision Systems and Instrumentation, Fairfax, VA). Following SCI the mice were housed individually. Baytril (25 mg/kg, Bayer, Toronto, Ontario, Canada) and buprenorphine (0.01 mg/kg, Schering-Plough, Hertfordshire, UK) were injected subcutaneously for 3 days post-SCI. Bladders were manually emptied twice daily for the duration of the experiment.

Behavioral Testing

Locomotor recovery of the animals was assessed by two blinded observers using the Basso Mouse Scale (BMS) open field locomotor score (Basso et al., 1995). The day following SCI, all mice were evaluated for any signs of locomotor recovery in their hindlimbs and mice that had BMS scores >0.5 were excluded from further analyses (four *Sox9* conditional knock-outs and five controls). Animals were evaluated once a week for 14 weeks after SCI. Left and right hind limb scores were averaged to generate a composite score. In addition, locomotion was evaluated at 14 weeks post-SCI using rodent activity boxes (Accuscan Instruments Inc, Columbus, OH). Activity boxes record the distance traveled by detecting breaks in a series of infrared light beams. The total distance traveled by each mouse was measured over a 2-h period at night (during their normal awake circadian cycle).

Spinal Cord Sectioning

Protein expression levels of SOX9 target genes were assessed at 14 weeks post-SCI. Animals were deeply anesthetized with 100 mg/kg ketamine: 5 mg/kg xylazine, and cardiac perfusion was carried out with 20 mL of saline at pH 7.4 followed by 20 mL 4% paraformaldehyde (4% PFA in 0.1 M phosphate buffer at pH 7.4). Spinal cords were dissected and postfixed for 2 h in 4% PFA followed by cryoprotection in 20% sucrose in 0.1 M phosphate buffer at pH 7.4 at 4°C overnight. Spinal cords were embedded in Tissue-Tek O.C.T. Compound (Sakura Finetek U.S.A. Inc., Torrance, CA), frozen over dry ice, and stored at −80°C overnight. Frozen cords were then cross-sectioned at 16 μm using a cryostat, and serially thaw-mounted on Superfrost™ glass slides (Fisher Scientific Company, Ottawa, Canada).

Immunohistochemistry and Trichrome Staining

Immunohistochemistry was conducted using the primary antibodies listed in Table 2. Slides were incubated with the appropriate dilutions of primary antibodies in a humidified chamber at 4°C overnight. Sections were stained for CSPG expression using the monoclonal antibody CS56 that recognizes the terminal portions of chondroitin sulfate-4 or -6 side chains and thus detects a variety of CSPGs (Avnur and Geiger, 1984). The CS56 was detected with a biotinylated goat anti-mouse IgM (Vector laboratories, Burlingame, CA) secondary antibody (1:200). Sections were then incubated for 45 min with avidin-peroxidase conjugate (Elite Kit, Vector laboratories, Burlingame, CA) at room temperature, and the signal visualized by peroxidase diaminobenzine (DAB, Invitrogen, Carlsbad, CA). Sections to be stained for perineuronal nets (PNNs) were washed in PBS 3 × 10 min, and incubated with biotinylated Wisteria Floribunda Lectin (WFA, Sigma Aldrich, St. Louis, MO) (1:1,000) for 1 h at room temperature. Sections were then incubated for 45 min with avidin-peroxidase conjugate (Elite Kit, Vector laboratories, Burlingame, CA) at room temperature, and the signal visualized by peroxidase diaminobenzine (DAB, Invitrogen, Carlsbad, CA). All DAB staining was conducted with a 2 min DAB reagent incubation time for all *Sox9* conditional knock-out and control cord sections, and were completed at the same time. Immunofluorescent labeling of the remaining proteins was performed using the following secondary antibodies; Alexa-Fluor 488-conjugated goat anti-mouse IgG (1:500, Invitrogen, Carlsbad, CA), Alexa-Fluor 488-conjugated goat anti-rabbit IgG (1:500, Invitrogen, Carlsbad, CA), or Alexa-Fluor 594-conjugated goat anti-rabbit IgG (1:500, Invitrogen, Carlsbad, CA), for 1 h at room temperature. Slides were then washed in PBS and coverslipped with ProLong Gold Anti-Fade mounting medium (Invitrogen, Carlsbad, CA). Gomori's Trichrome staining was used to stain for collagen according to the manufacturer's instructions (HT10316, Sigma Aldrich, St. Louis, MO).

Quantification of GFAP, CS56, Trichrome, NF-200, 5-HT, and WFA Staining

GFAP, CS56, trichrome, and NF-200 staining was analyzed as follows: 16 μm thick cross-sections 160 μm apart between 1.6 mm rostral through 1.6 mm caudal to the epicenter of injury were analyzed for positive staining using Image Pro Plus software (Media Cybernetics Inc, Bethesda, MD). A threshold was set for each stained section that identified positive signal (staining above background levels). The area of positive staining was normalized to total cord area. Staining results were grouped into five bins based on position relative to the lesion epicenter that was arbitrarily set as zero. The bin set as the epicenter encompassed 0.65 mm rostral and 0.65 mm caudal to the epicenter. The 1.3 mm included in the "epicenter" bin approximates the size of the head of the impactor. The rostral bins encompassed two directly adjacent segments of spinal cord rostral to the lesion (0.8 mm each) and the two caudal bins encompassed two directly adjacent segments of spinal cord caudal to the lesion (0.8 mm each).

The area of 5-HT immunoreactivity (area per area of interest) was quantified in the intermediolateral cell column (IML) and in the ventral horns in 16 μm thick cross-sections 160 μm apart obtained 0.8 to 1.6 mm caudal to the injury site using Image Pro Plus Software (Media Cybernetics Inc, Bethesda, MD). A single preset area was used to define all IML or ventral horn regions in all cords across both *Sox9* conditional knock-out and control animal

sections. The area of positive 5-HT immunoreactivity was quantified within this set area defined as the IML or ventral horn. The area of WFA immunoreactivity to identify PNNs was analyzed using 16 μm thick cross-sections 160 μm apart sampled at T10. Positive staining was quantified using Image Pro Plus Software (Media Cybernetics Inc, Bethesda, MD) using a threshold which identified positive signal (staining above background levels).

Statistical Analysis

Mean values are expressed ±SE. Both *in vitro* and *in vivo* mRNA analyses were subjected to statistical analysis using Student's *t*-test; 5-HT and WFA quantification was subjected to statistical analysis using Student's *t*-test. CS56, trichrome, GFAP, and NF-200 immunohistochemical quantification was subjected to statistical analysis using two way ANOVA with Neuman-Keuls *post hoc* test at each binned region of the cord, rostral, epicenter, and caudal to the site of injury. BMS results were subjected to statistical analysis using two-way repeated measures ANOVA with a Neuman-Keuls *post hoc* test. Activity Box locomotion was subjected to statistical analysis using one-way ANOVA with Neuman-Keuls *post hoc* test. Analyses were conducted with GraphPad Prism software (GraphPad Software Inc, La Jolla, CA), except for two-way ANOVAs which were conducted with SigmaStat software (Systat Software Inc, San Jose, CA), and significance was accepted at $P < 0.05$. A two-way ANOVA summary table is provided as Supporting Information Table 1.

RESULTS

Changes in Gene Expression in Primary Astrocytes Isolated from *Sox9* Conditional Knock-Outs

Astrocyte cultures were isolated from *Sox9* conditional knock-out and from control mice to evaluate the effects of *Sox9*-ablation on gene expression in primary astrocytes. These cultures were treated with 4-hydroxytamoxifen for 1 week and then cultured free of tamoxifen for an additional week before harvesting for RNA isolation. Using quantitative-PCR (Q-PCR) we measured the mRNA levels of *Sox9, Xt-1, Xt-2, C4st-1, Col2a1, Col4a1,* cartilage link protein *(Crtl),* and aggrecan *(Agc)* (Fig. 1). The mRNA levels of glial fibrillary acidic protein *(Gfap),* a marker of astrocyte activation, and brevican and neurocan (two CSPG core proteins) were also measured as we predicted that SOX9 would regulate genes broadly associated with astrocyte activation and scar production. Quantitative PCR demonstrated that administration of 4-hydroxytamoxifen resulted in a 72% ± 4% reduction in *Sox9* mRNA expression compared with control mouse astrocyte cultures. Reduced *Sox9* expression was associated with a statistically significant reduction in the expression of *Xt-1, Agc,* brevican, neurocan, *Col2a1,* and *Gfap,* in comparison with control astrocyte cultures (Fig. 1). Control astrocyte cultures treated with vehicle alone (no tamoxifen) did not show any reductions in SOX9 target gene expression.

Changes in Gene Expression in the Injured Spinal Cord in *Sox9* Conditional Knock-Outs

To determine if the reductions in gene expression observed in the $Sox9^{flox/flox};Cre$ primary astrocyte cultures would also be observed after SCI we evaluated mRNA expression levels at the lesion in *Sox9* conditional knock-out and control mouse spinal cords 1 week after a 70 kdyne SCI. Q-PCR demonstrated a 62 ± 11% reduction in *Sox9* mRNA levels in the *Sox9*

conditional knock-out mice compared with controls (Fig. 2). This reduction in *Sox9* mRNA levels was associated with a statistically significant reduction in *Xt-1, C4st-1, Agc,* brevican, neurocan, *Col2a1, Col4a1,* and *Gfap* mRNA expression compared with control mice (Fig. 2). To determine if these changes in mRNA levels resulted in parallel changes in protein levels we evaluated protein expression by western and slot blot analysis. *Sox9* conditional knock-out mice displayed significantly reduced SOX9, GFAP, and CSPG protein expression 2 weeks post-SCI (Fig. 3).

Sox9 Conditional Knock-Out Mice Demonstrate Improved Locomotor Recovery After SCI

As the glial scar in general and CSPGs in particular have been identified as inhibitors of axonal regeneration after SCI we predicted that the reduction in CSPG and collagen expression at the spinal lesion observed at 1 to 2 weeks postinjury would lead to improved locomotor recovery in *Sox9* conditional knock-out mice. $Sox9^{flox/flox}$, *Cre,* and control mice were administered tamoxifen for 1 week and allowed a week for tamoxifen washout before undergoing a 70 kdyne SCI using the Infinite Horizon impactor. Hind limb function was evaluated weekly for 14 weeks post-SCI. Day 1 following SCI all mice displayed paralyzed hind limbs, scoring a zero on the Basso Mouse Scale (BMS). In both *Sox9* conditional knock-out and control mice hind limb locomotion gradually improved over time. Locomotor BMS scoring in control mice reached a plateau of 0.63 ± 0.21 at 4 weeks post-SCI, (Fig. 4a). The median BMS score in this group of 0.5 indicates slight (less than 90°) movement in one ankle. In contrast, the BMS scores of the *Sox9* conditional knock-out mice continued to improve past 4 weeks and did not reach a plateau until 11 weeks post-SCI, achieving an average BMS score of 1.81 ± 0.19. The median BMS score for *Sox9* conditional knock-out mice of 2 indicates extensive (greater than 90°) movement in both ankles. The significantly higher scores of the *Sox9* conditional knock-out mice were accompanied by a statistically significant increase in ability to achieve plantar placement of their hind limbs (χ^2 test $P = 0.005$); six of nine *Sox9* conditional knock-out mice displayed at least one hind limb capable of plantar placement compared with 1 of 11 control mice which were capable of plantar placement. Finally, *Sox9* conditional knock-out mice and controls were placed in a computer-monitored rodent activity box to record total distance traversed over a 2 h period. Fourteen weeks after SCI, control mice covered a total distance of 1,414 ± 269 cm in 2 h, whereas *Sox9* conditional knock-out mice covered a total distance of 3,481 ± 814 cm in 2 h. The distance traversed by the *Sox9* conditional knock-out mice was significantly greater than that in the injured control animals and was not significantly different from uninjured $Sox9^{flox/flox}$ mice (3,330 ± 402 cm in 2 h) or uninjured control mice (3,452 ± 526.5 cm in 2 h) ($P = 0.027$ by one-way ANOVA with Neuman-Keuls *post hoc* test) (Fig. 4b).

Sox9 Conditional Knock-Out Mice Display Reduced CSPG, Collagen, and GFAP Expression at the Lesion Site 14 Weeks Following SCI

Since the *Sox9* conditional knock-out animals had reduced levels of *Xt-1, C4st-1, Agc,* brevican, neurocan, *Col2a1, Col4a1,* and *Gfap* mRNA at 1 week post-SCI and concomitant reductions in CSPG and GFAP protein levels at the lesion 2 weeks post-SCI, we anticipated that these animals would display reduced evidence of a glial scar at 14 weeks post-SCI. Spinal cord sections from *Sox9* conditional knock-out mice at 14 weeks after SCI demonstrated a significant reduction in CSPG immunoreactivity (area immunoreactivity per

cord area) rostral to, caudal to and at the lesion epicenter compared with controls (Fig. 5). The area of CSPG immunoreactivity was inversely correlated with BMS scores by linear regression analysis ($r^2 = 0.69$). Quantifying the area of positive trichrome staining for collagen (blue stain in Fig. 6) demonstrated reduced amounts of collagen (area immunoreactivity per cord area) in the lesion epicenter in *Sox9* conditional knock-out mice compared to controls. Finally, in agreement with the Q-PCR data at 1 week post-SCI and the protein quantitation at 2 weeks post-SCI, immunohistochemistry demonstrated reduced expression of GFAP (area immunoreactivity per cord area) in *Sox9* conditional knock-out mice rostral, caudal and at the lesion epicenter 14 weeks postinjury (Fig. 7).

Sox9 Conditional Knock-Out Mice have Increased Neurofilament-Positive Fibers in the Penumbra of the Lesion Site Following SCI

As the reduced CSPG and collagen levels in the *Sox9* conditional knock-out lesions would be predicted to correlate with an environment more permissive to axonal growth and sprouting, we expected to observe an increased number of neurofilament-positive fibers in the spinal lesions of the *Sox9* conditional knock-out mice compared with controls. Immunostaining spinal cord sections from *Sox9* conditional knock-outs and controls for neurofilament-200 immunoreactivity demonstrated significant reductions in neurofilament at their lesion epicenters compared with more rostral and caudal levels in both genotypes. Although the area of neurofilament-200 immunoreactivity (area immunoreactivity per cord area) in the *Sox9* conditional knock-out mice was not significantly different from controls at the lesion epicenter, neurofilament immunoreactivity was increased in the bins 0.8 mm rostral and caudal to the lesion epicenter in *Sox9* conditional knock-outs compared with controls (Fig. 8).

Sox9 Knock-Out Mice Display Increased 5-HT Immunoreactivity Caudal to the Lesion Site Following SCI

Descending serotonergic (5-HT positive) projections from the raphe nuclei control a variety of normal body functions. Serotonergic projections synapsing in the dorsal horn modulate pain sensation (Bardin et al., 2000; Calejesan et al., 1998), serotonergic projections targeting sympathetic preganglionic neurons in the intermediolateral cell column (IML) contribute to autonomic regulation (Allen and Cechetto, 1994), and serotonergic projections synapsing in the ventral horn provide excitatory input to motor neurons, the loss of which correlates with locomotor dysfunction (Saruhashi et al., 1996). To evaluate whether the improved recovery achieved by the *Sox9* conditional knock-out mice could be attributed to increased 5-HT inputs onto targets caudal to the injury we performed immunostaining for 5-HT on cross-sections from *Sox9* conditional knock-outs and controls 14 weeks after SCI. Between 0.8 mm and 1.6 mm caudal to the lesion epicenter *Sox9* conditional knock-out mice displayed a statistically significant increase in 5-HT immunoreactivity in the IML and ventral horn, compared with control mice (Fig. 9).

Sox9 Conditional Knock-Out Mice Display Decreased WFA Caudal to the Lesion Site Following SCI

In addition to their contribution to the glial scar matrix CSPGs are also a major component of the PNN ECM that stabilize synapses during development (Galtrey and Fawcett, 2007)

and limit plasticity in the adult nervous system. Since *Sox9* conditional knock-outs demonstrated reduced levels of CSPGs and other ECM components at the glial scar we evaluated whether they may also demonstrate reductions in the ECM in their PNNs. Cross-sections from *Sox9* conditional knock-outs and controls were stained with biotinylated Wisteria floribunda agglutinin (WFA). WFA binds *N*-acetylgalactosamine side chains in proteoglycans including CSPGs (Celio and Blumcke, 1994; Hartig et al., 1992). Cross-sections 1.6 to 3.2 mm caudal of the lesion epicenter were selected for WFA-staining to determine whether conditional *Sox9* ablation might lead to a reduction in PNN ECM distal to the lesion. WFA staining revealed a reduction in PNNs in the *Sox9* knock-out mice caudal to the lesion compared with control mice 14 weeks post SCI (Fig. 10).

DISCUSSION

Although the glial scar plays a key role in the acute response to SCI by sealing the lesion site, restoring homeostasis, and modulating immunity, it also presents an obstacle to recovery by limiting structural plasticity (Rolls et al., 2009). The antiregenerative properties of the glial scar are predominantly caused by the build-up of various proteoglycans and collagens after injury (Stichel and Muller, 1998; Stichel et al., 1999a, b). Having previously demonstrated that siRNA knock-down of the transcription factor SOX9 down-regulates the expression of CSPG-synthetic enzymes in astrocyte cultures (Gris et al., 2007), we investigated the effect of *in vivo Sox9* conditional knock-out on gene expression, glial scarring, and functional recovery after SCI.

In addition to our siRNA work demonstrating SOX9 regulation of *Xt-1*, *Xt-2*, and *C4st-1* (Gris et al., 2007), others have shown that SOX9 also regulates the expression of *Col2a1* (Lefebvre et al., 1997, 1998), *Col4a1* (Sumi et al., 2007), the CSPG core protein *Agc* (Sekiya et al., 2000), and *Crtl* (Kou and Ikegawa, 2004); 4-hydroxytamoxifen-induced knock-down of *Sox9* expression in astrocyte cultures was accompanied by reduced mRNA expression of most of the predicted SOX9 target genes. In the injured spinal cord of tamoxifen-treated $Sox9^{flox/flox};Cre$ mice the mRNA expression of these same genes with the addition of *C4st-1* and *Col4a1* were also significantly reduced compared with controls; this was paralleled by reductions in SOX9, GFAP, and CSPG protein levels. These results largely confirm the anti-*Sox9* siRNA results in rat primary astrocytes previously reported (Gris et al., 2007) and demonstrate that the SOX9 target genes identified in astrocyte cell culture experiments are also regulated by SOX9 *in vivo* in the injured spinal cord.

Some predicted SOX9 target genes did not show reduced expression in *Sox9* knock-out astrocyte cultures or spinal cord-injured mice. *Xt-2* expression was not reduced in either the $Sox9^{flox/flox};Cre$ astrocyte cultures or spinal cord injured mice, suggesting that SOX9 activity is not necessary for the expression of this isoform of xylosyltransferase. The reduction of *Xt-2* expression that we previously described in rat primary astrocyte cultures may simply reflect a minor species difference in SOX9 activities between rats and mice. Although *C4st-1* expression was not reduced in $Sox9^{flox/flox};Cre$ astrocyte cultures it was reduced in the injured spinal cords of $Sox9^{flox/flox};Cre$ mice. This may reflect *in vitro* versus *in vivo* differences in the regulation of *C4st-1* gene expression. The greater dependence *C4st-1* expression on SOX9 activity in the injured spinal cord may be due to the large

increase in SOX9 expression that occurs within the first 12 h of SCI that may mask the effects of other regulators that are important to *C4st-1* expression *in vitro*. Expression of *Col4a1*, like *C4st-1*, was not reduced in the *Sox9* conditional knock-out astrocyte cultures but was reduced in the spinal lesions of *Sox9* conditional knock-out mice after SCI. Others have shown that collagen 4 is expressed in the lesion epicenter in a directly adjacent but nonoverlapping pattern with the GFAP-positive astrocytes in the surrounding penumbra (Klapka and Muller, 2006). Together this suggests that SOX9 is required for the expression of *Col4a1* in the cells (likely meningeal fibroblasts) that produce collagen 4 in the lesion epicenters but not in astrocytes. Finally *Crtl* expression was not reduced in the *Sox9* conditional knock-out cultures or in the *Sox9* conditional knock-out mice after SCI suggesting that SOX9 activity is not necessary for *Crtl* expression. This result was surprising as others have demonstrated that anti-*Sox9* siRNA transfection into a human chondrosarcoma cell line, OUMS-27, resulted in reduced levels of *Crtl* expression (Kou and Ikegawa, 2004). However, this same group also demonstrated the presence of a SOX9-independent enhancer element in the 5′-UTR of the *Crtl* gene. Thus we suggest that this SOX9 independent enhancer element may be regulating expression of *Crtl* in astrocyte cultures and in the injured spinal cord.

The *Sox9* conditional knock-out mice achieved significantly higher BMS scores than controls, improved rates of plantar placement and traversed two to three times the distance traversed by controls 14 weeks post-SCI. The strong correlation ($r^2 = 0.61$) between BMS scores at 14 weeks post-SCI and decreased area of CSPG staining at the lesion site suggests that the improved locomoter function in the *Sox9* conditional knock-outs is due to the decreased CSPG expression in these mice following SCI. The reduced expression of *Xt-1*, *C4st-1*, *Agc*, brevican, neurocan, *Col2a1*, and *Col4a1* would be expected to produce a less fibrous scar with less CSPG content. Gomori's trichrome staining 14 weeks postinjury confirmed that the *Sox9* conditional knock-out lesions had less collagen than controls. Immunohistochemistry further demonstrated that there was less CSPG content in the *Sox9* conditional knock-out lesions than controls. Neurofilament immunostaining showed that the area of neurofilament immunoreactivity at the lesion epicenter did not differ significantly between *Sox9* conditional knock-outs and controls. This suggests that the improved locomotor recovery in *Sox9* conditional knock-outs is not due to a greater degree of axonal sparing in these mice nor is it likely due to greater numbers of axons traversing the lesion site to connect caudal to the lesion. However, neurofilament immunostaining rostral and caudal to the lesion epicenters was increased in the *Sox9* conditional knock-out mice, consistent with the suggestion that the reduced CSPG content in the penumbra of the *Sox9* conditional knock-outs permits greater amounts of axonal sprouting. Axonal sprouting rostral and caudal to the lesion may allow the formation of connections with spared propriospinal neurons and underlie the improved locomotor behavior in the *Sox9* conditional knock-outs.

CSPG immunoreactivity and WFA-staining demonstrate reduced CSPG expression and PNN matrix rostral and caudal to the penumbra 14 weeks post-SCI in the *Sox9* conditional knock-outs. Evidence suggests that CSPGs are up-regulated within PNNs both near and far from a CNS lesion (Massey et al., 2006). Enzymatic digestion of PNNs by chondroitinase ABC leads to reactivation of plasticity in adult animals (Corvetti and Rossi, 2005; Pizzorusso et

al., 2002), and enhances spared fiber collateral sprouting and synapse formation in injured animals (Tropea et al., 2003). Thus reduced *Sox9* expression may open a window for increased plasticity following SCI at denervated sites within and remote to the lesion. In the *Sox9* conditional knock-outs, reduced PNNs and CSPG content in the PNNs may have permitted spared propriospinal or descending supraspinal axons to synapse on deafferented targets caudal to the lesion. Evidence in support of this comes from the 5-HT immunostaining which clearly showed increased 5-HT immunoreactivity caudal to the lesion around the IML and ventral horn in *Sox9* conditional knock-outs.

The postulate that reduced CSPGs in the PNNs distal to the lesion may account for the improved locomotor recovery observed in the *Sox9* conditional knock-outs might explain other facets of the recovery in these mice. For example the *Sox9* conditional knock-outs have higher BMS scores than controls starting at 1 week post-SCI. This improvement in locomotor activity seems to occur too quickly to be explained by long-range regeneration of inputs rostral to the lesion. The absence of increased neurofilament immunoreactivity at the lesion epicenter also argues against any significant amount of regeneration or sparing across the lesion epicenter in the *Sox9* knock-outs. However, short-range sprouting of spared axons onto deafferented targets promoted by reduced CSPGs in PNNs would be expected to occur rapidly. This type of repair may also be less prone to miswiring of circuits as the most likely axons to form new synapses on a target will be those that are already innervating adjacent neurons in the same field.

A second possible explanation for improved locomotor recovery of the *Sox9* conditional knock-outs may be the reduced GFAP expression in these mice after SCI. The identification of GFAP as part of a battery of genes upregulated by SOX9 after SCI suggests that SOX9 not only upregulates the expression of ECM-related genes but also regulates the overall state of astrocyte activation and response to injury. In addition to being a major producer of the glial scar, astrocytes also play an important role in inflammation. In response to TGF-β1 astrocytes up-regulate expression of the proinflammatory genes nitric oxide synthase-2 (NOS-2) and cyclooxygenase-2 (COX-2) (Hamby et al., 2008). IL-1β and TNF-α also increase astrocyte production of nitric oxide (Hamby et al., 2008; Hewett et al., 1993). In the *Sox9* conditional knock-out mice, reduced GFAP expression might indicate less astrocyte activation and perhaps less production of proinflammatory mediators. Thus a muted inflammatory response may account for some of the improved recovery observed in the *Sox9* conditional knock-outs.

A third possible explanation for improved locomotor recovery of the *Sox9* conditional knock-outs rests on evidence that SOX9 may play a role in neural stem differentiation. Expression studies have shown that SOX9 is expressed by neuroepithelial cells in the ventricular zone of the developing spinal cord, by oligodendrocytes and by astrocytes but not by neurons (Stolt et al., 2003). Knocking out *Sox9* in the developing mouse spinal cord results in perinatal lethality, decreased numbers of oligodendrocyte progenitors and astrocytes and an increased number of motor neurons (Stolt et al., 2003) and neuroblasts (Scott et al., 2010). MicroRNA studies also suggest that SOX9 is gliogenic, promoting neural stem cells to adopt an astrocyte or oligodendrocyte fate (Cheng et al., 2009). Following injury, neural stem cells proliferate and differentiate almost exclusively into

astrocytes (Johansson et al., 1999; Meletis et al., 2008) that generate scar, but not into neurons (Johansson et al., 1999). These results are consistent with the hypothesis that, in neural stem cells, SOX9 expression promotes a glial rather than a neuronal cell fate and that, in *Sox9* conditional knock-outs, neural stem cells activated by the injury may adopt a neuronal as opposed to a glial fate. If astrocytes newly-born after injury contribute to CSPG production, or if newly-born neuroblasts are able to generate new neurons or produce growth factors that support neuronal survival (Behrstock et al., 2006; Llado et al., 2004; Madhavan et al., 2008), then the effect of *Sox9* ablation on neural stem cell behavior (decreasing the number of newborn astrocytes and increasing the number of neuroblasts or neurons) may explain the improved recovery of *Sox9* conditional knock-out mice after SCI. This possibility is being evaluated by fate mapping studies in the *Sox9* conditional knock-outs after SCI.

In summary, *Sox9* conditional knock-out improved hind limb motor function in mice following T9 SCI. The improved recovery in the *Sox9* conditional knock-outs correlated with reduced levels of GFAP, collagen, and CSPG expression at the lesion and at sites distant from the lesion. We suggest that the reduced CSPG expression at the glial scar and in PNNs distant to the injury opened up a window of opportunity for increased local plasticity possibly allowing for the formation of new propriospinal connections or sprouting from spared axons onto deafferented targets. This explanation is consistent with the neurofilament immunoreactivity showing increased fiber sprouting in the lesion penumbra but no increase in fibers that traverse the lesion epicenter. It is also consistent with the demonstrated reduction in PNNs caudal to the lesion and increased 5-HT immunoreactivity demonstrating more serotonergic inputs onto IML and ventral horn targets caudal to the lesion. These results suggest that inhibition of SOX9 activity may be a novel therapeutic strategy for the treatment of SCI.

Acknowledgments

The authors gratefully acknowledge the technical assistance of Anna Pniak.

Grant sponsors: Canadian Institutes of Health Research (CIHR), International Foundation of Research in Paraplegia (IFP), Natural Sciences and Engineering Research Council of Canada (NSERC) (to W.M.M.), and Foundation Recherche Medicale (to A.S.).

References

Akiyama H, Chaboissier MC, Martin JF, Schedl A, de Crombrugghe B. The transcription factor Sox9 has essential roles in successive steps of the chondrocyte differentiation pathway and is required for expression of Sox5 and Sox6. Genes Dev. 2002; 16:2813–2828. [PubMed: 12414734]

Alilain WJ, Horn KP, Hu H, Dick TE, Silver J. Functional regeneration of respiratory pathways after spinal cord injury. Nature. 2011; 475:196–200. [PubMed: 21753849]

Allen GV, Cechetto DF. Serotoninergic and nonserotoninergic neurons in the medullary raphe system have axon collateral projections to autonomic and somatic cell groups in the medulla and spinal cord. J Comp Neurol. 1994; 350:357–366. [PubMed: 7533797]

Avnur Z, Geiger B. Immunocytochemical localization of native chondroitin-sulfate in tissues and cultured cells using specific monoclonal antibody. Cell. 1984; 38:811–822. [PubMed: 6435883]

Bahr M, Przyrembel C, Bastmeyer M. Astrocytes from adult rat optic nerves are nonpermissive for regenerating retinal ganglion cell axons. Exp Neurol. 1995; 131:211–220. [PubMed: 7895822]

Bardin L, Schmidt J, Alloui A, Eschalier A. Effect of intrathecal administration of serotonin in chronic pain models in rats. Eur J Pharmacol. 2000; 409:37–43. [PubMed: 11099698]

Basso DM, Beattie MS, Bresnahan JC. A sensitive and reliable locomotor rating scale for open field testing in rats. J Neurotrauma. 1995; 12:1–21. [PubMed: 7783230]

Behrstock S, Ebert A, McHugh J, Vosberg S, Moore J, Schneider B, Capowski E, Hei D, Kordower J, Aebischer P, et al. Human neural progenitors deliver glial cell line-derived neurotrophic factor to parkinsonian rodents and aged primates. Gene Therapy. 2006; 13:379–388. [PubMed: 16355116]

Bi W, Huang W, Whitworth DJ, Deng JM, Zhang Z, Behringer RR, de Crombrugghe B. Haploinsufficiency of Sox9 results in defective cartilage primordia and premature skeletal mineralization. Proc Natl Acad Sci USA. 2001; 98:6698–6703. [PubMed: 11371614]

Bradbury EJ, Moon LD, Popat RJ, King VR, Bennett GS, Patel PN, Fawcett JW, McMahon SB. Chondroitinase ABC promotes functional recovery after spinal cord injury. Nature. 2002; 416:636–640. [PubMed: 11948352]

Calejesan AA, Ch'ang MH, Zhuo M. Spinal serotonergic receptors mediate facilitation of a nociceptive reflex by subcutaneous formalin injection into the hindpaw in rats. Brain Research. 1998; 798:46–54. [PubMed: 9666072]

Celio MR, Blumcke I. Perineuronal nets--A specialized form of extracellular matrix in the adult nervous system. Brain Res Brain Res Rev. 1994; 19:128–145. [PubMed: 8167657]

Cheng LC, Pastrana E, Tavazoie M, Doetsch F. miR-124 regulates adult neurogenesis in the subventricular zone stem cell niche. Nat Neurosci. 2009; 12:399–408. [PubMed: 19287386]

Condic ML, Snow DM, Letourneau PC. Embryonic neurons adapt to the inhibitory proteoglycan aggrecan by increasing integrin expression. J Neurosci. 1999; 19:10036–10043. [PubMed: 10559411]

Corvetti L, Rossi F. Degradation of chondroitin sulfate proteoglycans induces sprouting of intact purkinje axons in the cerebellum of the adult rat. J Neurosci. 2005; 25:7150–7158. [PubMed: 16079397]

David S, Lacroix S. Molecular approaches to spinal cord repair. Annu Rev Neurosci. 2003; 26:411–440. [PubMed: 12626698]

Davies SJ, Fitch MT, Memberg SP, Hall AK, Raisman G, Silver J. Regeneration of adult axons in white matter tracts of the central nervous system. Nature. 1997; 390:680–683. [PubMed: 9414159]

Davies SJ, Goucher DR, Doller C, Silver J. Robust regeneration of adult sensory axons in degenerating white matter of the adult rat spinal cord. J Neurosci. 1999; 19:5810–5822. [PubMed: 10407022]

Dou CL, Levine JM. Inhibition of neurite growth by the NG2 chondroitin sulfate proteoglycan. J Neurosci. 1994; 14:7616–7628. [PubMed: 7996200]

Eddleston M, Mucke L. Molecular profile of reactive astrocytes-Implications for their role in neurologic disease. Neuroscience. 1993; 54:15–36. [PubMed: 8515840]

Fawcett JW, Asher RA. The glial scar and central nervous system repair. Brain Res Bull. 1999; 49:377–391. [PubMed: 10483914]

Friedlander DR, Milev P, Karthikeyan L, Margolis RK, Margolis RU, Grumet M. The neuronal chondroitin sulfate proteoglycan neurocan binds to the neural cell adhesion molecules Ng-CAM/L1/NILE and N-CAM, and inhibits neuronal adhesion and neurite outgrowth. J Cell Biol. 1994; 125:669–680. [PubMed: 7513709]

Galtrey CM, Fawcett JW. The role of chondroitin sulfate proteoglycans in regeneration and plasticity in the central nervous system. Brain Res Rev. 2007; 54:1–18. [PubMed: 17222456]

Garcia-Alias G, Barkhuysen S, Buckle M, Fawcett JW. Chondroitinase ABC treatment opens a window of opportunity for task-specific rehabilitation. Nat Neurosci. 2009; 12:1145–1151. [PubMed: 19668200]

Gris P, Murphy S, Jacob JE, Atkinson I, Brown A. Differential gene expression profiles in embryonic, adult-injured and adult-uninjured rat spinal cords. Mol Cell Neurosci. 2003; 24:555–567. [PubMed: 14664807]

Gris P, Tighe A, Levin D, Sharma R, Brown A. Transcriptional regulation of scar gene expression in primary astrocytes. Glia. 2007; 55:1145–1155. [PubMed: 17597120]

Hamby ME, Hewett JA, Hewett SJ. TGF-beta1 reduces the heterogeneity of astrocytic cyclooxygenase-2 and nitric oxide synthase-2 gene expression in a stimulus-independent manner. Prostaglandins Other Lipid Mediat. 2008; 85:115–124. [PubMed: 18194875]

Hartig W, Brauer K, Bruckner G. Wisteria floribunda agglutinin-labelled nets surround parvalbumin-containing neurons. Neuroreport. 1992; 3:869–872. [PubMed: 1421090]

Hayashi S, McMahon AP. Efficient recombination in diverse tissues by a tamoxifen-inducible form of Cre: A tool for temporally regulated gene activation/inactivation in the mouse. Dev Biol. 2002; 244:305–318. [PubMed: 11944939]

Hewett SJ, Corbett JA, McDaniel ML, Choi DW. Interferon-gamma and interleukin-1 beta induce nitric oxide formation from primary mouse astrocytes. Neurosci Lett. 1993; 164:229–232. [PubMed: 7512249]

Houle JD, Tom VJ, Mayes D, Wagoner G, Phillips N, Silver J. Combining an autologous peripheral nervous system “bridge” and matrix modification by chondroitinase allows robust, functional regeneration beyond a hemisection lesion of the adult rat spinal cord. J Neurosci. 2006; 26:7405–7415. [PubMed: 16837588]

Johansson CB, Momma S, Clarke DL, Risling M, Lendahl U, Frisen J. Identification of a neural stem cell in the adult mammalian central nervous system. Cell. 1999; 96:25–34. [PubMed: 9989494]

Karimi-Abdolrezaee S, Eftekharpour E, Wang J, Schut D, Fehlings MG. Synergistic effects of transplanted adult neural stem/progenitor cells, chondroitinase, and growth factors promote functional repair and plasticity of the chronically injured spinal cord. J Neurosci. 2010; 30:1657–1676. [PubMed: 20130176]

Klapka N, Muller HW. Collagen matrix in spinal cord injury. J Neurotrauma. 2006; 23:422–435. [PubMed: 16629627]

Kou I, Ikegawa S. SOX9-dependent and -independent transcriptional regulation of human cartilage link protein. J Biol Chem. 2004; 279:50942–50948. [PubMed: 15456769]

Lefebvre V, Huang W, Harley VR, Goodfellow PN, de Crombrugghe B. SOX9 is a potent activator of the chondrocyte-specific enhancer of the pro alpha1(II) collagen gene. Mol Cell Biol. 1997; 17:2336–2346. [PubMed: 9121483]

Lefebvre V, Li P, de Crombrugghe B. A new long form of Sox5 (L-Sox5), Sox6 and Sox9 are coexpressed in chondrogenesis and cooperatively activate the type II collagen gene. EMBO J. 1998; 17:5718–5733. [PubMed: 9755172]

Lemons ML, Howland DR, Anderson DK. Chondroitin sulfate proteoglycan immunoreactivity increases following spinal cord injury and transplantation. Exp Neurol. 1999; 160:51–65. [PubMed: 10630190]

Llado J, Haenggeli C, Maragakis NJ, Snyder EY, Rothstein JD. Neural stem cells protect against glutamate-induced excitotoxicity and promote survival of injured motor neurons through the secretion of neurotrophic factors. Mol Cell Neurosci. 2004; 27:322–331. [PubMed: 15519246]

Madhavan L, Ourednik V, Ourednik J. Neural stem/progenitor cells initiate the formation of cellular networks that provide neuroprotection by growth factor-modulated antioxidant expression. Stem Cells. 2008; 26:254–265. [PubMed: 17962704]

Massey JM, Hubscher CH, Wagoner MR, Decker JA, Amps J, Silver J, Onifer SM. Chondroitinase ABC digestion of the perineuronal net promotes functional collateral sprouting in the cuneate nucleus after cervical spinal cord injury. J Neurosci. 2006; 26:4406–4414. [PubMed: 16624960]

McKeon RJ, Schreiber RC, Rudge JS, Silver J. Reduction of neurite outgrowth in a model of glial scarring following CNS injury is correlated with the expression of inhibitory molecules on reactive astrocytes. J Neurosci. 1991; 11:3398–3411. [PubMed: 1719160]

Meiners S, Powell EM, Geller HM. A distinct subset of tenascin/CS-6-PG-rich astrocytes restricts neuronal growth in vitro. J Neurosci. 1995; 15:8096–8108. [PubMed: 8613745]

Meletis K, Barnabe-Heider F, Carlen M, Evergren E, Tomilin N, Shupliakov O, Frisen J. Spinal cord injury reveals multilineage differentiation of ependymal cells. PLoS Biol. 2008; 6:e182. [PubMed: 18651793]

Milev P, Friedlander DR, Sakurai T, Karthikeyan L, Flad M, Margolis RK, Grumet M, Margolis RU. Interactions of the chondroitin sulfate proteoglycan phosphacan, the extracellular domain of a

receptor-type protein tyrosine phosphatase, with neurons, glia, and neural cell adhesion molecules. J Cell Biol. 1994; 127:1703–1715. [PubMed: 7528221]

Pizzorusso T, Medini P, Berardi N, Chierzi S, Fawcett JW, Maffei L. Reactivation of ocular dominance plasticity in the adult visual cortex. Science. 2002; 298:1248–1251. [PubMed: 12424383]

Reier PJ, Houle JD. The glial scar: Its bearing on axonal elongation and transplantation approaches to CNS repair. Adv Neurol. 1988; 47:87–138. [PubMed: 3278533]

Rolls A, Shechter R, Schwartz M. The bright side of the glial scar in CNS repair. Nat Rev Neurosci. 2009; 10:235–241. [PubMed: 19229242]

Saruhashi Y, Young W, Perkins R. The recovery of 5-HT immunoreactivity in lumbosacral spinal cord and locomotor function after thoracic hemisection. Exp Neurol. 1996; 139:203–213. [PubMed: 8654523]

Schmalfeldt M, Bandtlow CE, Dours-Zimmermann MT, Winterhalter KH, Zimmermann DR. Brain derived versican V2 is a potent inhibitor of axonal growth. J Cell Sci. 2000; 113:807–816. [PubMed: 10671370]

Scott CE, Wynn SL, Sesay A, Cruz C, Cheung M, Gomez Gaviro MV, Booth S, Gao B, Cheah KS, Lovell-Badge R, Briscoe J. SOX9 induces and maintains neural stem cells. Nat Neurosci. 2010; 13:1181–1189. [PubMed: 20871603]

Sekiya I, Tsuji K, Koopman P, Watanabe H, Yamada Y, Shinomiya K, Nifuji A, Noda M. SOX9 enhances aggrecan gene promoter/enhancer activity and is up-regulated by retinoic acid in a cartilage-derived cell line, TC6. J Biol Chem. 2000; 275:10738–1044. [PubMed: 10753864]

Silver J, Miller JH. Regeneration beyond the glial scar. Nat Rev Neurosci. 2004; 5:146–156. [PubMed: 14735117]

Stichel C, Muller H. Experimental strategies to promote axonal regeneration after traumatic central nervous system injury. Prog Neurobiol. 1998; 56:119–148. [PubMed: 9760698]

Stichel CC, Hermanns S, Luhmann HJ, Lausberg F, Niermann H, D'Urso D, Servos G, Hartwig HG, Muller HW. Inhibition of collagen IV deposition promotes regeneration of injured CNS axons. Eur J Neurosci. 1999a; 11:632–646. [PubMed: 10051764]

Stichel CC, Lausberg F, Hermanns S, Muller HW. Scar modulation in subacute and chronic CNS lesions: Effects on axonal regeneration. Restor Neurol Neurosci. 1999b; 15:1–15. [PubMed: 12671239]

Stolt CC, Lommes P, Sock E, Chaboissier MC, Schedl A, Wegner M. The Sox9 transcription factor determines glial fate choice in the developing spinal cord. Genes Dev. 2003; 17:1677–1689. [PubMed: 12842915]

Sumi E, Iehara N, Akiyama H, Matsubara T, Mima A, Kanamori H, Fukatsu A, Salant DJ, Kita T, Arai H, Doi T. SRY-related HMG box 9 regulates the expression of Col4a2 through transactivating its enhancer element in mesangial cells. Am J Pathol. 2007; 170:1854–1864. [PubMed: 17525254]

Tropea D, Caleo M, Maffei L. Synergistic effects of brain-derived neurotrophic factor and chondroitinase ABC on retinal fiber sprouting after denervation of the superior colliculus in adult rats. J Neurosci. 2003; 23:7034–7044. [PubMed: 12904464]

Wang D, Ichiyama RM, Zhao R, Andrews MR, Fawcett JW. Chondroitinase combined with rehabilitation promotes recovery of forelimb function in rats with chronic spinal cord injury. J Neurosci. 2011; 31:9332–9344. [PubMed: 21697383]

Yamada H, Fredette B, Shitara K, Hagihara K, Miura R, Ranscht B, Stallcup WB, Yamaguchi Y. The brain chondroitin sulfate proteoglycan brevican associates with astrocytes ensheathing cerebellar glomeruli and inhibits neurite outgrowth from granule neurons. J Neurosci. 1997; 17:7784–7795. [PubMed: 9315899]

Zuo J, Neubauer D, Dyess K, Ferguson TA, Muir D. Degradation of chondroitin sulfate proteoglycan enhances the neurite- promoting potential of spinal cord tissue. Exp Neurol. 1998; 154:654–662. [PubMed: 9878200]

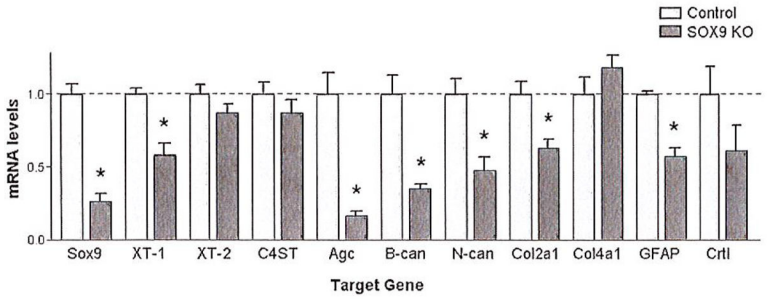

Fig. 1.

Astrocytes from *Sox9* conditional knock-out mice demonstrate reduced glial scar gene expression compared with control mice. Treating $Sox9^{flox/flox};Cre$ astrocyte cultures with 1 μM 4-hydroxytamoxifen for 1 week results in a 72 ± 4% reduction in *Sox9* mRNA levels and is accompanied by a statistically significant reduction in *Xt-1,* aggrecan (Age), brevican (B-can) neurocan (N-can), *Col2A1,* and *Gfap* mRNA levels compared to $Sox9^{flox/flox}$ astrocytes treated with 1 μM 4-hydroxytamoxifen, ($P < 0.05$, Student's *t*-test; $n = 4$ per group).

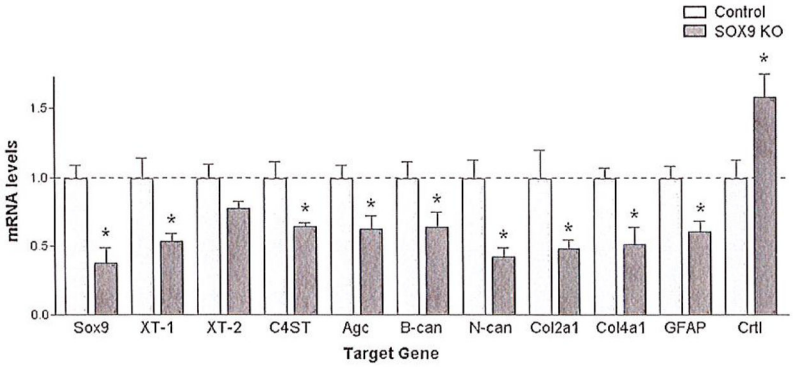

Fig. 2.

Sox9 conditional knock-out mice demonstrate reduced glial scar gene expression compared with control mice. Spinal cord-injured, tamoxifen-treated $Sox9^{flox/flox};Cre$ mice demonstrate a 62 ± 11% reduction in *Sox9* mRNA expression compared with spinal cord-injured, tamoxifen-treated $Sox9^{flox/flox}$ mice 1 week post-SCI. This reduction in *Sox9* expression is associated with a statistically significant reduction in *Xt-1, C4st-1, Age, brevican* (B-can), *neurocan* (N-can), *Col2A1* and *4A1,* and *GFAP* mRNA levels ($P < 0.05$, Student's *t-test; n =* 5 per group).

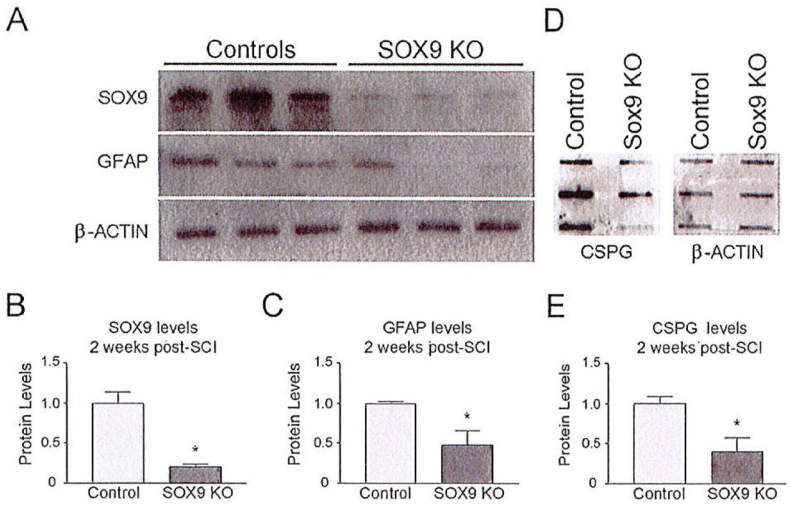

Fig. 3.

Sox9 conditional knock-out mice demonstrate reduced SOX9, GFAP, and CSPG protein 2 weeks post-SCI. (**A**) Western blot analysis and subsequent densitometry (**B, C**) demonstrate reduced SOX9 and GFAP levels in *Sox9* conditional knock-out mice in comparison with control mice (normalized to β-actin levels) ($P \leq 0.05$, Student's *t*-test; $n = 3$). (**D**) Slot blot and subsequent densitometry (**E**) demonstrates reduced CSPG expression in *Sox9* conditional knock-out mice compared with controls (normalized to β-actin levels) ($P \leq 0.05$, Student's *t*-test; $n = 3$).

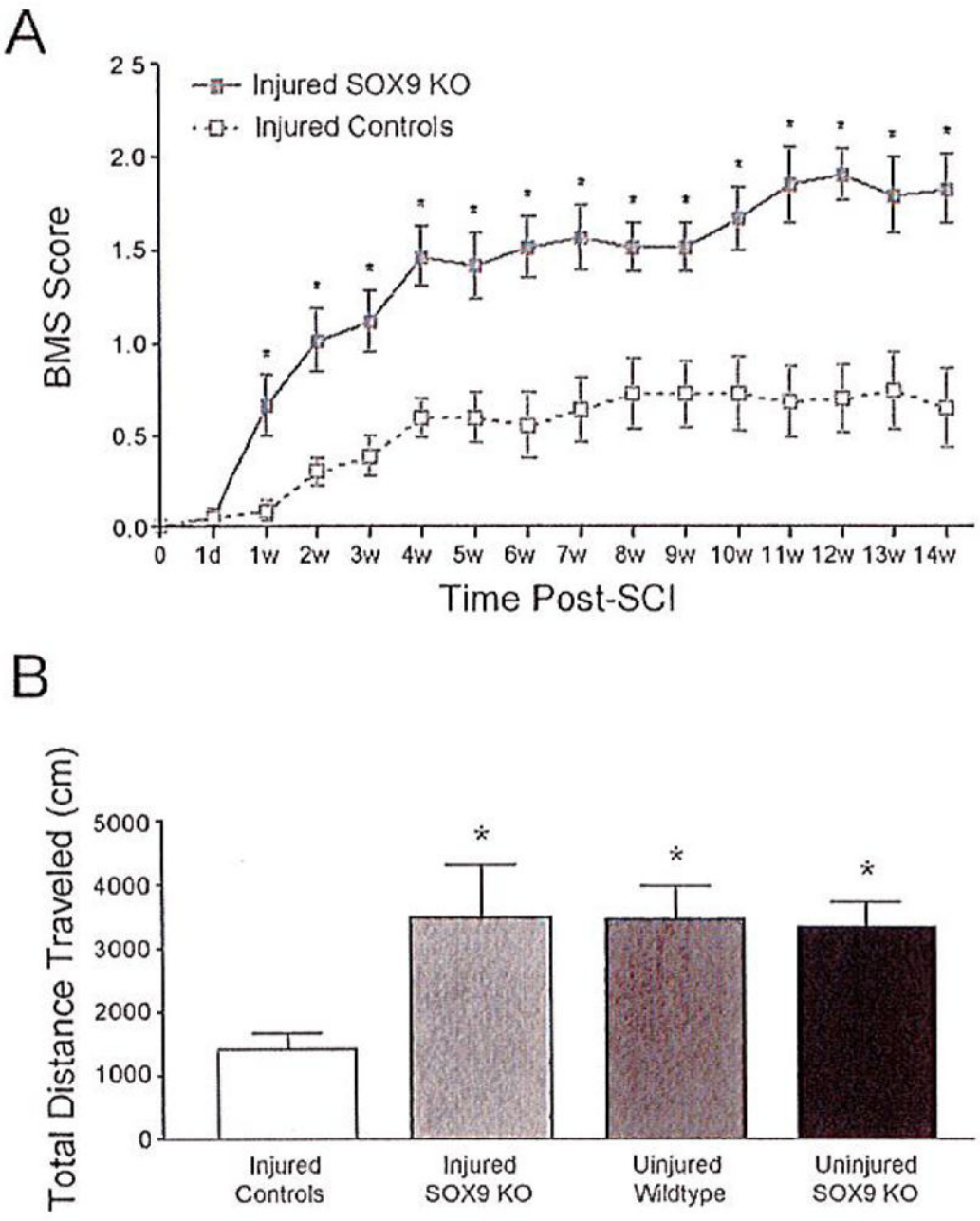

Fig. 4.

Sox9 conditional knock-out mice demonstrate improved locomotor recovery after SCI. (**A**) *Sox9* conditional knock-out mice display increased hind limb functional recovery in comparison with control mice. Both *Sox9* conditional knock-out and control mice display hind limb paralysis immediately following SCI. *Sox9* conditional knock-out mice score higher (increased hind limb function) on the Basso Mouse Scale (BMS) in comparison with control mice every week between 1 and 14 weeks after SCI ($P < 0.05$, two-way repeated measures ANOVA, Newman-Keuls *post hoc* tests ($P < 0.05$); $n = 9$ *Sox9* KO, $n = 11$ control). (**B**) *Sox9* conditional knock-out mice demonstrate increased distance traveled in

comparison with control injured mice measured over a 2 h period in a rodent activity box ($P < 0.05$, one-way ANOVA; $n = 9$ *Sox9* K0, $n = 11$ controls).

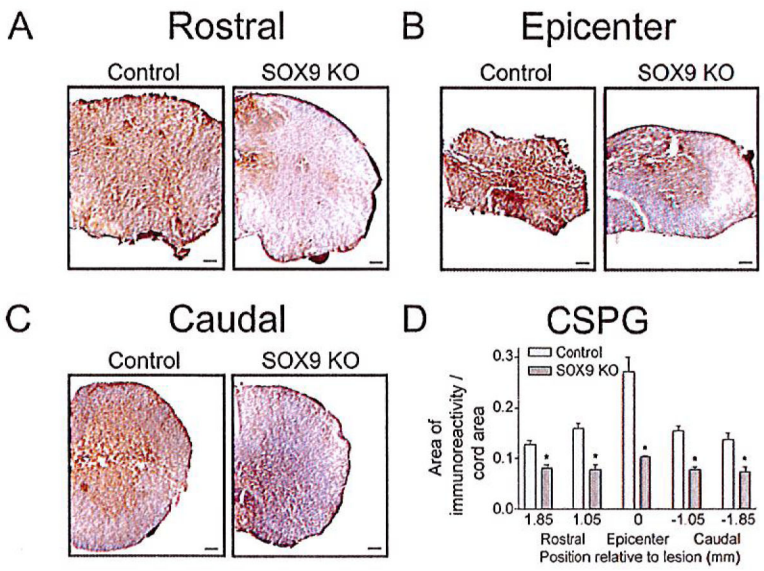

Fig. 5.

Sox9 conditional knock-out mice display reduced CSPG expression 14 weeks post-SCI. Representative photomicrographs of anti-CSPG DAB immunohistochemical staining approximately 1 mm rostral to the lesion epicenters (**A**) at the epicenters (**B**) and 1 mm caudal to the lesion epicenters (**C**) from *Sox9* conditional knock-outs and controls as indicated. Bar = 100 μm. (**D**) Quantification of area of CSPG immunoreactivity in *Sox9* conditional knock-out and control sections. The area of immunostaining per cross-sectional area of spinal cord was quantified using ImageProPlus software on sections spaced 160 μm apart. The area per area measurements were then grouped into bins centered on the positions indicated. The bin representing epicenter in each animal extended 0.65 mm rostral and caudal to the center of the lesion. The bins rostral and caudal to the epicenter were centered on the positions shown relative to the epicenter and included sections 0.4 mm rostral and caudal. *Statistically significantly different from controls ($P < 0.05$, two-way ANOVA, Newman-Keuls *post hoc* test ($P < 0.05$); $n = 9$ *Sox9* KO, $n = 11$ controls).

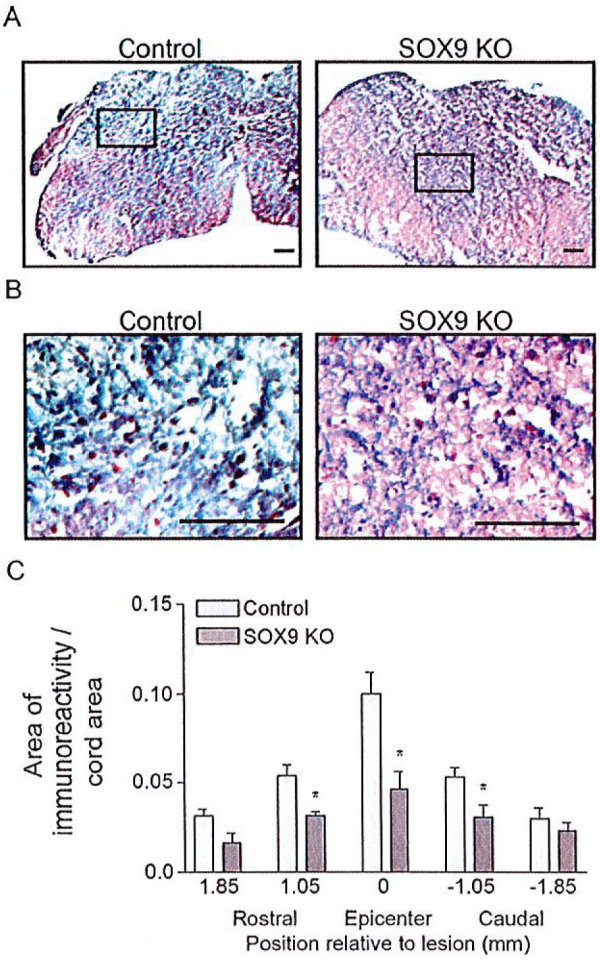

Fig. 6.

Sox9 conditional knock-out mice demonstrate reduced collagen at the lesion epicenter 14 weeks post-SCI. (**A**) Representative photomicrographs of Trichrome-stained spinal cord sections from the lesion epicenters of *Sox9* conditional knock-out and control mice. (**B**) High power magnifications of boxed areas in A). (**C**) Quantification of area of collagen (blue) staining in *Sox9* conditional knock-out and control sections. Areas of collagen staining were quantified as explained in legend to Figure 5. *Statistically significantly different from controls ($P < 0.05$, two-way ANOVA, Newman-Keuls *post hoc* test ($P < 0.05$); $n = 9$ *Sox9* KO, $n = 11$ control). Bars = 100 μm.

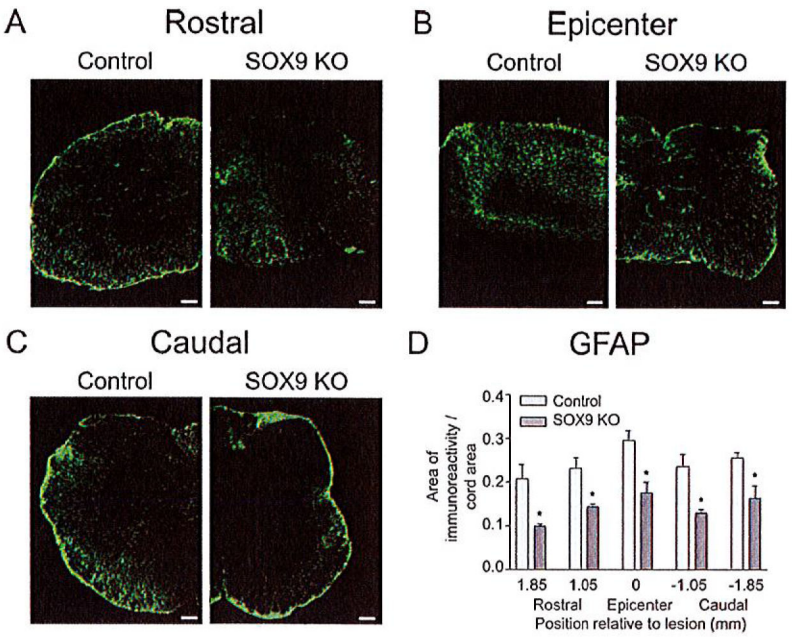

Fig. 7.

Sox9 conditional knock-out mice demonstrate reduced GFAP expression 14 weeks post-SCI. (**A**) Representative photomicrographs of anti-GFAP immunostaining from spinal cord sections approximately 1 mm rostral to the lesion epicenters (A) at the epicenters (**B**) and 1 mm caudal to the lesion epicenters (**C**) from *Sox9* conditional knock-outs and controls as indicated. (**D**) Quantification of area of GFAP immunoreactivity (area per area) in *Sox9* conditional knock-out and control sections. Areas of GFAP immunostaining were quantified as explained in legend to Figure 5. *Statistically significantly different from controls ($P < 0.05$, two-way ANOVA, Newman-Keuls *post hoc* test ($P < 0.05$); $n = 9$ *Sox9* KO, $n = 11$ controls). Bars = 100 μm.

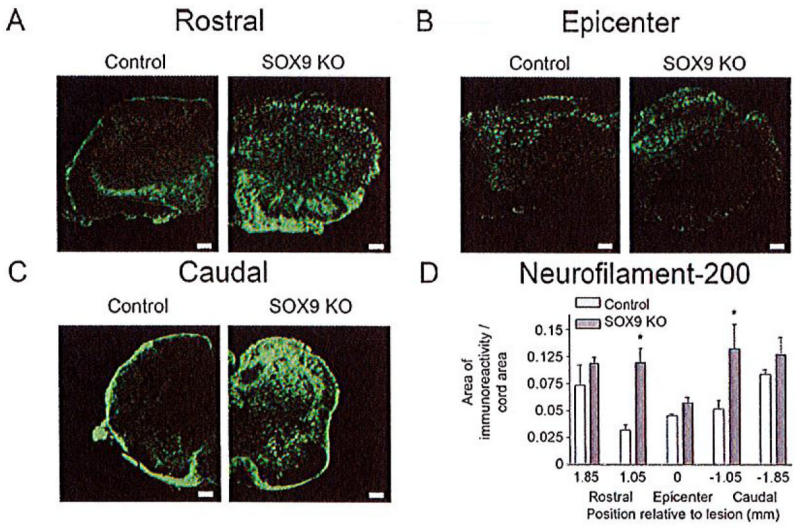

Fig. 8.

Sox9 conditional knock-out mice demonstrate increased neurofilament immunoreactivity rostral and caudal to their lesion epicenters 14 weeks post-SCI. (**A**) Representative photomicrographs of anti-neurofilament immunostaining from spinal cord sections approximately 0.5 mm rostral to the lesion epicenters (A) at the epicenters (**B**) and 0.5 mm caudal to the lesion epicenters (**C**) from *Sox9* conditional knock-outs and controls as indicated. (**D**) Quantification of area of neurofilament immunoreactivity (area per area) in *Sox9* conditional knock-out and control sections. Areas of neurofilament immunostaining were quantified as explained in legend to Figure 5. *Statistically significantly different from controls ($P < 0.05$, two-way ANOVA, Newman-Keuls *post hoc* test ($P < 0.05$); $n = 9$ *Sox9* KO, $n = 11$ control). Bars = 100 μm.

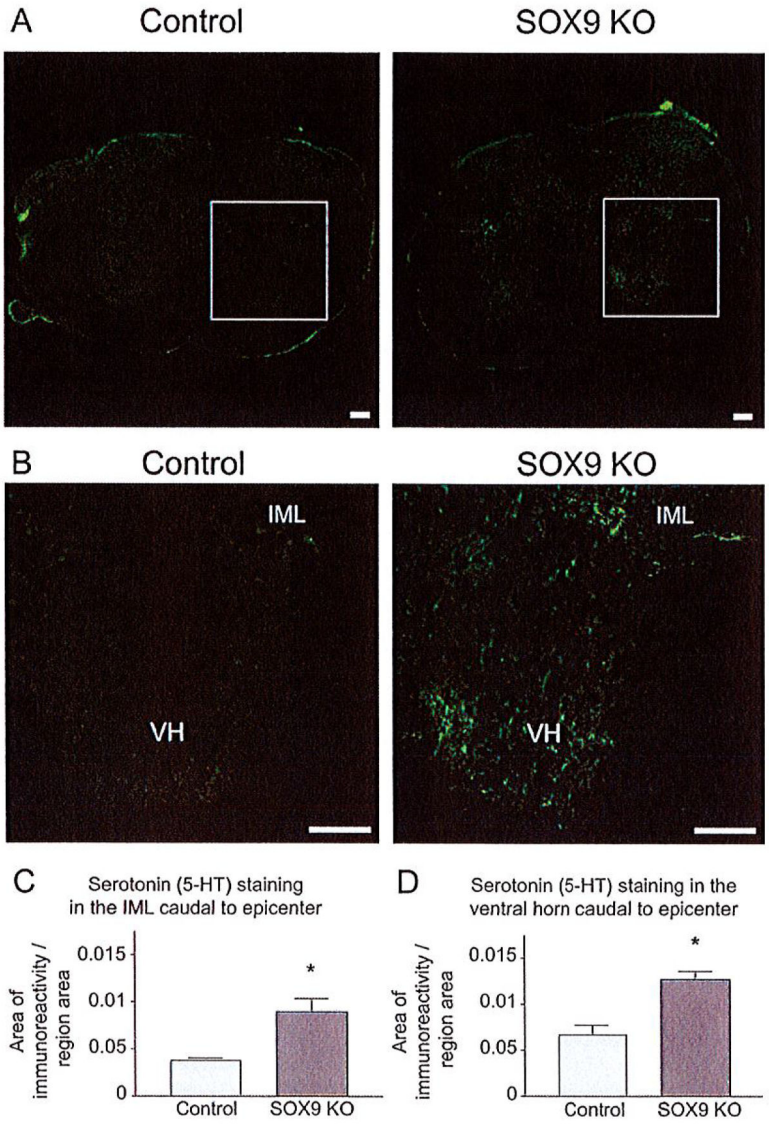

Fig. 9.

Sox9 conditional knock-out mice display increased 5-HT immunoreactivity caudal to the lesion. Immunohistochemistry was used to detect serotonin in the spinal cord 14 weeks post-SCI. (**A**) Representative photomicrographs of sections stained for 5-HT immunoreactivity ~ 1.2 mm caudal to the lesion epicenter from *Sox9* conditional knock-out and control mice. Almost no 5-HT immunoreactivity was observed caudal to the lesion in control mice; however, 5-HT immunoreactivity was observed caudal to the lesion in *Sox9* KO mice. (**B**) High power magnifications of boxed areas in A). Quantification of 5-HT immunoreactivity. 5-HT-immunoreactivity was significantly increased in intermediolateral (IML) (**C**) cell column and the ventral horn (VH) (**D**) of *Sox9* conditional knock-out mice in comparison to control mice. *Statistically significantly different from controls (Student's *t*-test, $P \leq 0.05$; $n = 9$ *Sox9* KO, $n = 11$ controls). Bar = 100 μm.

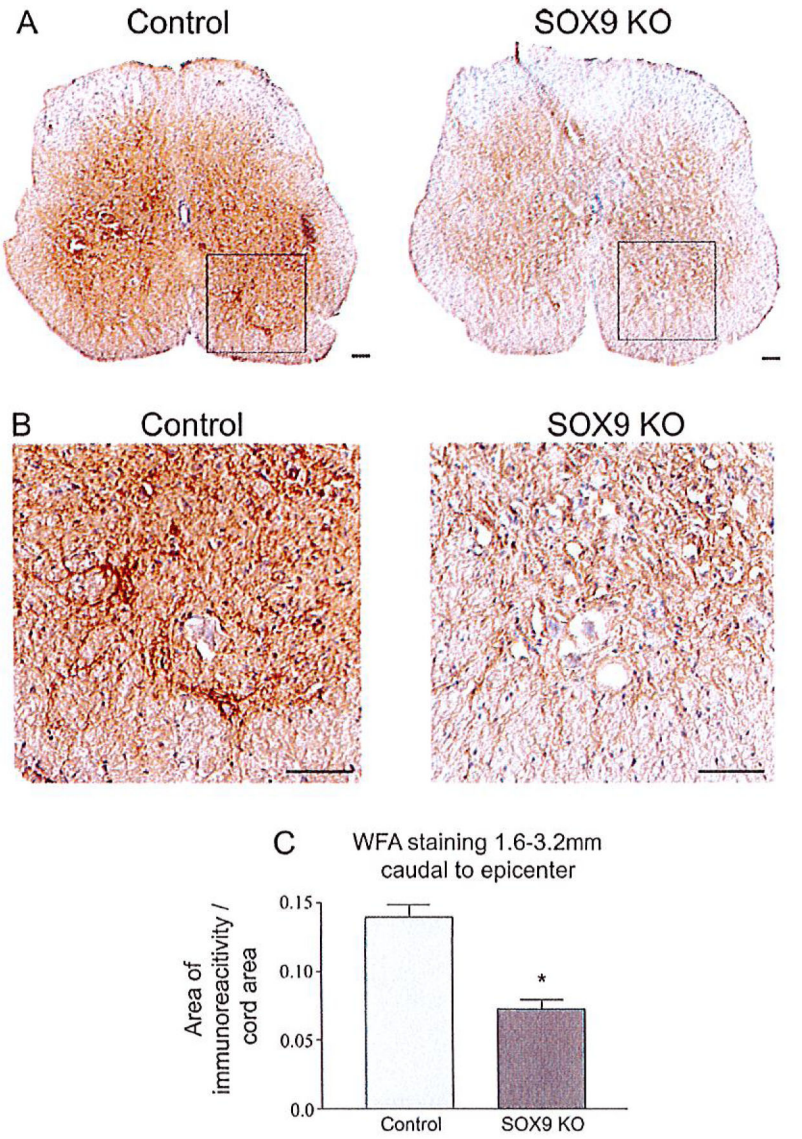

Fig. 10.

Perineuronal net (PNN) matrix is reduced in *Sox9* conditional knock-out mice caudal to the lesion 14 weeks post-SCI. WFA staining was used to detect PNN matrix caudal to lesion epicenter in control and *Sox9* conditional knock-out mice. (**A**) Representative photomicrographs of sections stained for WFA caudal to the lesion epicenter from *Sox9* conditional knock-out and control mice. (**B**) High power magnifications of boxed areas in A). (**C**) Quantification of area of WFA staining in *Sox9* conditional knock-out and control sections. The area of WFA-stained tissue per cross-sectional area of spinal cord was quantified using ImageProPlus software on sections spaced 160 μm apart from 1.6 to 3.2 mm caudal to the epicenters. *Statistically significantly different from controls (Student's *t*-test, $P \leq 0.05$; $n = 9$ *Sox9* KO, $n = 11$ controls).

TABLE 1

List of TaqMan Real-Time PCR Primer Probe Sets

Primer Probe	Catalog number	*PCR Ct range*
18s	4308329	*14.72–16.07*
Sox9	Mm00448840_m1	*21.88–23.64*
XT-I	Mm00558690_m1	*27.34–29.57*
XT-II	Mm00461181_m1	*24.72–25.87*
C4st-1	Mm00517563_m1	*21.72–23.01*
Aggrecan	Mm00545807_m1	*24.53–27.07*
Brevican	Mm00476090_m1	*18.35–21.70*
Neurocan	Mm00484007_m1	*17.31–20.73*
Collagen 2A1	Mm01309562_g1	*23.40–27.33*
Collagen 4A1	Mm00802377_m1	*20.73–21.39*
GFAP	Mm01253033_m1	*19.96–22.16*
Cartilage link protein	Mm00488952_m1	*28.35–29.94*

TABLE 2

List of Primary Antibodies and Stains Used for Spinal Cord Staining

Antibody	Dilution	Isotype	*Source*
Anti-GFAP	1:500	Mouse IgG	*Millipore, Billerica, Massachusetts*
Anti-CS56	1:300	Mouse IgM	*Sigma Aldrich, St. Louis, Missouri*
Anti-NF200	1:1,000	Rabbit IgG	*Sigma Aldrich, St. Louis, Missouri*
Anti-5-HT	1:500	Rabbit IgG	*ImmunoStar, Hudson, Wisconsin*
VVFA	1:1,000		*Sigma Aldrich, St. Louis, Missouri*